The Strength of Steel Plates Subjected to Missile Impact

S. Ohte, H. Yoshizawa

Mechanical Engineering Research Laboratory,
Toshiba R & D Center, Toshiba Corporation,
Ukishima-cho 4-1, Kawasaki-shi 210, Japan

N. Chiba, S. Shida

Mechanical Engineering Research Laboratory, Hitachi, Ltd.,
Saiwai-cho 3-1-1, Hitachi-shi, Ibaraki-ken 317, Japan

SUMMARY

This paper describes test results in which steel plates were subjected to missile impact, and a new experimental formula to evaluate the steel plate strength. The objective of this study was to obtain experimental data for designing Primary Containment Vessels to withstand postulated missile impacts. In order to investigate the missile nose shape effect on steel plate strength and the target thickness dependence of critical energy for target plate fracture, a series of missile impact tests for steel plates has been carried out.

Materials for targets and missiles were carbon steel plate 7 - 38 mm thick and austenitic stainless steel, respectively. Cylindrical, semi-spherical and conical-nosed missiles were used in impact tests. Missile mass and velocity were 3 - 50 kg and 25 - 180 m/s, respectively. Loads at target support points and dynamic strains in the target have been measured. After the impact test, residual deformations in targets and missiles have been measured.

As shown in the test results, different kinds of target fracture mode were observed, according to missile nose shapes. In cylindrical missile impact tests, the target was only deformed when missile energy level was low, and was perforated when high. The critical missile energy, below which the target was not perforated, corresponds to values calculated from usual empirical formulas. However, target fracture (which means generating cracks or small hole in a target) occured for conical missiles at much lower energy level that these values.

Dynamic target and missile behavior and critical conditions for target plate fracture have been investigated from experimental data, with respect to dynamic strains in targets, residual deformations in targets and missiles.

From these results, a new empirical formula to evaluate the critical energy for target plate fracture E_f (J), applicable to three kinds of missiles, has been obtained, as shown below.

$$E_f = 2.9T^{1.5}D_e^{1.5}$$

$$D_e = \begin{cases} (1 + 2.9(\tan\frac{\theta}{2})^{2.1})\,T \cdots \text{for conical missiles} \\ D_m \cdots \text{ for cylindrical, spherical and conical (De > Dm) missiles} \end{cases}$$

where, T is target thickness (mm), D_m is missile diameter (mm), θ is nose angle of conical missile (degree).

1. Introduction

Various kinds of missile generation is assumed as one of postulated accidents that act upon a nuclear facility. The amount of damage this missile inflicts upon a primary containment vessel or other equipments is one of prime importance for nuclear reactor safety design.

Missiles are assumed to be generated as a result of aircraft accident, turbine fracture, reactor component fracture, etc. Missile parameters which affect target damage are considered to be mass, velocity, geometry etc. Vessels or equipments include concrete wall or steel plate, as a target to be considered for missile impact. Despite various studies conducted on this matter in the past, no adequate design basis data has been attained as yet, regarding nose shape effects of a missile on a steel plate.

In view of these circumstances, an experimental study has been conducted as a basic research for examining missile nose shape effects upon steel plate strength. Various experimental studies have been conducted up to the present regarding steel plate resistance against missile impact. BRL equation [1] or Stanford equation [2] is very familiar as a critical perforation condition for steel plate. Though this studies have been carried out referring to these empirical equations, it became clear, as a result, that a sharp nosed missile occasionally causes such damage as cracks or small hole, and that critical energy is very small and far from the value predicted by these equations.

This paper describes test results in which steel plates are subjected to variously shaped missile impacts, and a new formula to evaluate critical energy for steel plate integrity, which is applicable to cylindrical, semi-spherical and conical nosed missiles.

2. Test Methods

Materials for tested steel plates (later referred to as target) and missiles are carbon steel, JIS SGV49 and austenitic stainless steel, JIS SUS304, respectively. Mechanical properties of these materials are shown in Table 1. As is shown in Fig. 1, a 2 m x 2 m size target plate, is held against a backup structure, and is subjected to impact by a missile from a launcher. Target's dynamic strains, loads upon the support and missile velocity are measured by strain gauges, load cells and velocity detectors, respectively.

The missile involves three different nose shapes, including cylindrical, semi-spherical and conical shapes. Of these, the conical shaped missile further involves four different nose angles, including 90°, 40°, 30° and 20°.

Test conditions are listed in Table 2. Missile nose shape effects on critical energy for target fracture were investigated from results of tests on 7 and 20 mm thick targets. Target thickness effects on critical energy for target fracture were investigated from tests using 90° and 40° conical missiles.

3. Test Results

Test results for the 7 mm thick target are shown in Fig. 2. Test results have been classified according to the target failure modes. The following symbols are used in the figures in this paper.

    ○ : No failure - only plastic deformation, without cracks.

    △ : Fracture - Missile recoiled, leaving cracks or small hole.

    ✕ : Perforation - Missile passed through the target.

Photo. 1 shows a target perforated by a cylindrical missile. This is an example where the missile punched out a circular hole whose diameter is equal to the missile's own diameter by a shearing mechanism. In this case, critical perforation energy is mostly in good agreement with that predicted by three old equations shown in Fig. 2.

Contrarily, conical missile tests indicate that perforation could occur, even with smaller missile energy than that estimated by these equations. Either cracks or small hole are similarly generated at lesser energy than the perforation level. Thus, it becomes clear that critical fracture energy for a conical missile never agrees with values estimated by these equations. A target with cracks induced by a conical missile is shown in Photo. 2.

Though no critical fracture data for semi-spherical missile has been obtained, critical fracture energy is presumed to be almost the same magnitude as that of a cylindrical missile, based on target residual deformation observation.

Test results for a 20 mm thick target are shown in Fig. 3. It is clear that the critical energy for target fracture depends on the conical missile nose angle.

The results for 90° and 40° conical missiles are shown in Fig. 4. The symbol ● in Fig. 4(b) means the critical energy of 7 mm thick target for 40° conical missile, estimated by a simplified model analysis [3]. From Fig. 4, it becomes clear that the critical energy for target fracture for 90° and 40° conical missiles increases proportionally to the third power of target thickness, T.

4. Discussion

4-1 Dynamic Measurement Results

Dynamic strain in the plastic and elastic deformation area in a target and target supporting load are shown in Fig. 5. The following conclusions can be obtained from these data:

(1) Strain 1 curve indicates that plastic deformation is finished within $1 \sim 2$ ms after impact.

(2) A reaction force appears first at target supports $1 \sim 2$ ms after impact, and reaches its maximum in $6 \sim 8$ ms. After that, the load varies with a frequency of about 30 Hz, which agrees with that of strain 2, and with the eigen-frequency of the plate. Namely, a reaction force is found to be produced with target elastic vibration.

4-2 Target Plate Deformation and Fracture Modes

a) Deformation and Fracture Modes

Deformation and fracture modes, for target plate subjected to missile impact, are shown in Fig. 6. In case of cylindrical missile, the missile is not deformed. A round hole is punched through the target plate. The hole diameter is equal to the missile diameter D_M, as shown in Fig. 6(a). Because perforation occurs at the same time as an initial fracture is generated, no test result classified as fracture has been observed in cylindrical missile tests.

Contrarily, a conical missile nose is deformed into an almost flat shape with diameter, d_1, by compressive impact force, as shown in Fig. 6(b)(c). Where, d_2 means a contact area diameter between a target and a conical missile. The central portion of a target shows a significant reduction in thickness caused by a conical missile impact, and cracks initially appear around the area with diameter d_1. Secondary cracks are generated as the missile travels forward, pushing the target with its conical seat, if the missile energy level is

higher than the critical energy for target fracture.   Photo. 2 shows secondary cracks.

b) Fracture Condition of Target

Figure 7 shows the reduction in thickness and the strain through thickness for all the target plates tested with 90° conical missiles, that are classified as no-failure.   It can be concluded, from Fig. 7, that target fracture occurs when the strain through thickness reaches about 1.2 or when target thickness is reduced to about one third of the original thickness for 90° conical missiles.   Figure 8 shows similar results obtained from static compression tests, in which a 90° conical indenter has been used instead of 90° conical missile, as is shown in Fig. 9.   It becomes clear from, Fig. 7 and Fig. 8, that the critical reduction in thickness for target fracture in dynamic tests shows almost the same value as the thickness reduction in static tests.

c) Conical Missile Nose Deformation Behavior

The maximum residual deflection in target, W, and the flat shape diameter of conical missile nose, d_1, are shown in Fig. 10.   These data have been measured in tests whose results are classified as beeing no failure.   Though the maximum deflection in the target, W, increases proportionally to the missile energy, the flat shape diameter d_1 is independent of it. From these data, it is assumed that conical missile nose is deformed to a flat shape in a short time at collision.   After that, the target continues to deform until a crack is generated or until all the missile energy is absorbed.   As is shown in Fig. 6, an initial crack is generated around the flat area with diameter d_1, and target deformations vary according to the contact area size d_2 between target and conical missile.   So, it is thought reasonable that the critical energy for target fracture could be expressed as a function of diameters d_1 and d_2.

Diameter d_1 and d_2 dependences on target thickness are shown in Fig. 11.   Diameters d_1 and d_2 increase proportionally to target thickness T.   Diameter d_2 varies, depending on conical nose angle θ, whereas diameter d_1 is independent of this angle.   The new formula for the critical energy for target fracture, reflecting these results, will be discussed in the next paragraph.

4.3   New Critical Energy Formula for Target Fracture

In the following, an evaluation formula applicable even to a conical nosed missile is discussed.

Here, critical energy for target fracture, E_f (J) is assumed to be expressed by Eq. (1), similarly to the case of BRL equation, by analogy,

$$E_f \ (\equiv \tfrac{1}{2} M V_0^2) \ = \ C_1 \, T^{1.5} \, D_e^{1.5} \tag{1}$$

Where T is target thickness (mm) and D_e is missile equivalent diameter (mm), wherein $D_e = D_m$ (actual missile diameter) holds in case of a cylindrical missile.   Diameter, D_e, for a conical missile has been derived in the following manner.

In spite of the total contacting area between target and missile having a diameter d_2, as shown in Fig. 6, the location where a crack initially appears is closely related to a contacting section with the d_1 size smashed nose.

With these facts, Eq. (2), which is a combination of a term, representing d_1 effect but independent of θ, and a term that represents d_2 effect dependent on θ, is introduced for determining conical missile equivalent diameter D_e.

$$D_e \equiv d(T) + K(T, \theta) \tag{2}$$

As is indicated in Fig. 11, diameters d_1 and d_2 increase proportionally to target thickness T. Then, D_e should be expressed by Eq. (3).

$$D_e = C_2 T + K(\theta) T \tag{3}$$

As the second term in Eq. (3) represents the effect of an area where target and missile contact each other with its conical seat, as denoted d_2, the following condition will hold when characterizing the $K(\theta)$ property.

$K(\theta) \rightarrow 0 \qquad$ for $\qquad \theta \rightarrow 0$

$K(\theta) \rightarrow \infty \qquad$ for $\qquad \theta \rightarrow 180°$

Then, the following equation is adopted for diameter D_e,

$$D_e = C_2 T + C_3 (\tan\frac{\theta}{2})^n T \tag{4}$$

Wherein, as diameter, d_1 is almost equal to T, C_2 is assumed to be 1.

When critical fracture energy data for a cylindrical missile, shown in Fig. 2, and the same data for a conical missile, shown in Fig. 4, are substituted into Eqs. (1) and (4), the following constants are determined.

$$C_1 = 2.9, \quad C_3 = 2.9 \quad \text{and} \quad n = 2.1 \tag{5}$$

Regarding this equation, the assumption of $D_e = D_m$ is acceptable for a semi-spherical missile case, as its critical fracture energy hardly differs from that of a cylindrical missile. There is a case where the value D_e, derived from Eq. (4) for a conical missile having a large angle θ, becomes larger than D_m, but the same assumption of $D_e = D_m$ is also acceptable in such a case.

The new formula is summarized as Eq. (6).

$$E_f = 2.9 T^{1.5} D_e^{1.5}$$

$$D_e = \left\{ \begin{array}{l} T\{1 + 2.9(\tan\frac{\theta}{2})^{2.1}\} \quad \cdots \cdots \text{ for conical missiles} \\[2mm] D_m \quad \cdots \cdots \text{ for cylindrical, semi-spherical and conical } (D_e > D_m) \\ \qquad\qquad \text{missile} \end{array} \right\} \tag{6}$$

Critical energies for target fracture calculated from Eq. (6) are shown by the solid line in Figs. 3 and 4. The comparison between Eq. (6) and the test results for 7 mm thick target is shown in Fig. 12. From these figures, it is clear that Eq. (6) can closely represent all test results.

4. Conclusion

The following results have been obtained from a series of tests performed wherein cylindrical, semi-spherical and conical nose shaped missiles are impacted against a carbon steel plate ranging from 7 to 38 mm in thickness.
(1) Target fracture mode and critical fracture energy required significantly differ from each other, according to the missile's nose shape.
(2) Both critical fracture energy for cylindrical missile and that for semi-spherical missile mostly agree with values predicted by empirical equations generally used.

(3) Critical fracture energy for a conical missile is generally smaller than values predicted by empirical equations generally used.

(4) The following critical fracture energy, E_f (J) evaluation equation is obtained and is applicable to cylindrical, semi-spherical and conical missiles.

$$E_f = 2.9T^{1.5}D_e^{1.5}$$

$$D_e = \begin{cases} T\{1 + 2.9(\tan\frac{\theta}{2})^{2.1}\} \cdots\cdots \text{ for conical missiles} \\ D_m \cdots\cdots \text{ for cylindrical, semi-spherical and conical } (D_e > D_m) \\ \qquad\qquad \text{missile} \end{cases}$$

,where T is target thickness (mm), D_m in a missile diameter (mm) and θ is a nose angle of a conical missile (degree).

Acknowledgement
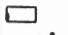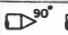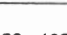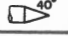
References

[1] WHITE, R. W. etc., "Containment of Fragments from a Runaway Reactor" Tech. Report No.6, SRIA-113, Sep. 1963.

[2] GWALTNEY, R. C., "Missile Generation and Protection in Light-Water-Cooled Power Reactor Plants", ORNL-NSIC-22, 1968.

[3] MIYAMOTO, H., SHIDA, S., CHIBA, N., OHTE, S., YOSHIZAWA, H., "Experimental Study on Strength of Steel Plates Subjected to Missile Impact.", J8-9, 5th SMiMT, 1979.

Table 1 Target and missile mechanical properties.

	Yield Stress (MPa),(kgf/mm²)	Tensile Strength (MPa),(kgf/mm²)	Elongation (%)	Reduction of Area (%)
SGV 49	343 , 35	490 , 50	40	75
SUS 304	284 , 29	637 , 65	80	80

Table 2 Test conditions.

Target Thickness (mm)	Missile			
	Nose Shape	Diameter (mm)	Mass (kg)	Velocity (m/s)
7	▭ ▭ ▷90° ▷40°	87.5	3~18	25~170
10	▷90°	66~160	3~50	50~180
20	▷90° ▷40° ▷30° ▷20°	66~160	3~50	50~150
30	▷90° ▷40°	66~160	4~50	60~150
38	▷40°	99~160	24~45	93~142

Fig. 1 Test method.

Fig. 2 Test results for a 7 mm thick target plate.

- x Perforation
- △ Cracks or Small Hole
- ○ Deformation Only

- Stanford Eq.
- Jacob De Marre Eq.
- BRL Eq.
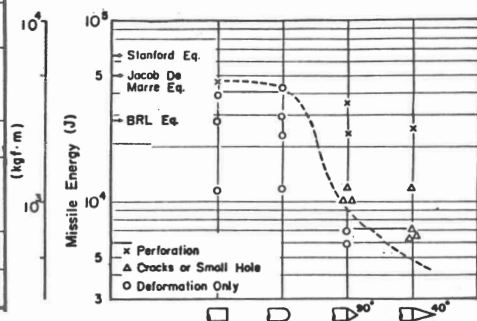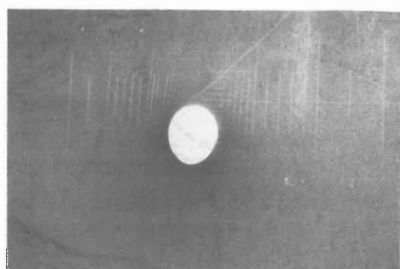
Photo. 1 Target perforated by a cylindrical missile.
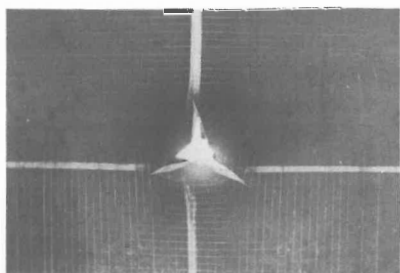
Photo. 2 Target fractured by a 90° conical missile.
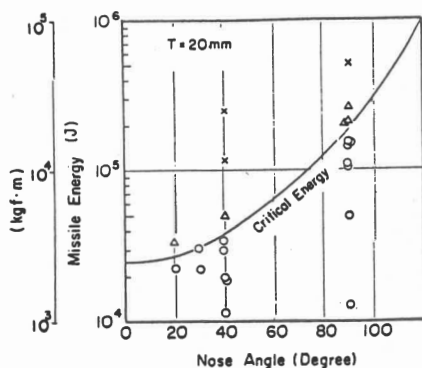
Fig. 3 Test results for a 20 mm thick target plate, when missile's conical nose is parametrically changed.
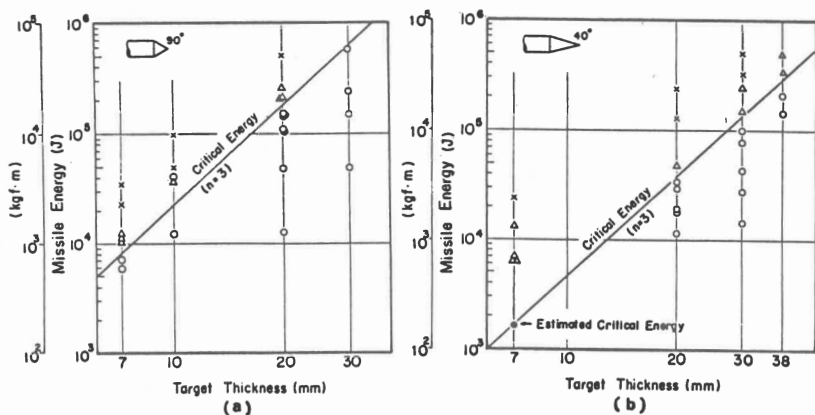
Fig. 4   Test results by use of 90° and 40° conical missiles.
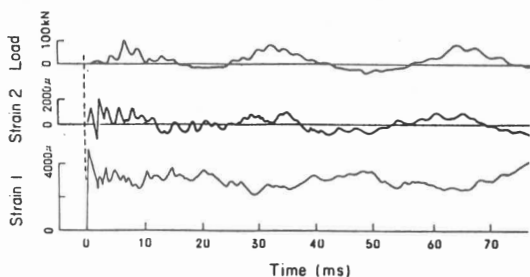

Fig. 5   Target dynamic strain and support load
when a 7 mm thick target plate is subjected
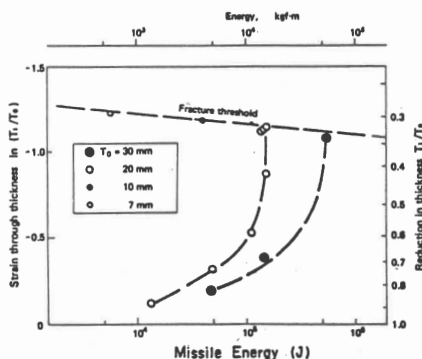to a 90° conical missile impact.

Fig. 7   Reduction in target plate thickness
for 90° conical missile
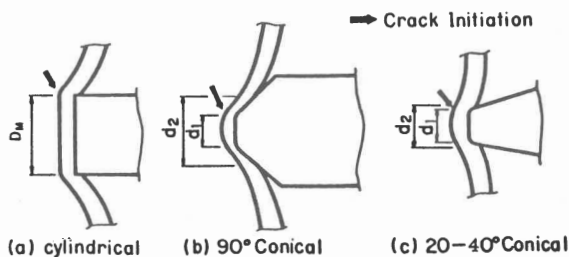(T_0: Thickness before test,
T_1: Minimum thickness after test).

Fig. 6   Target deformation mode and crack initiation location.
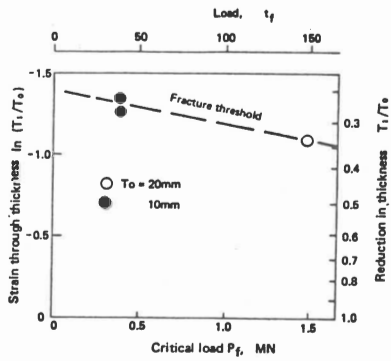
Fig. 8   Reduction in target plate thickness
after static compression   test by
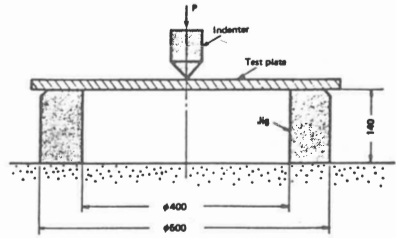a 90° conical indenter.

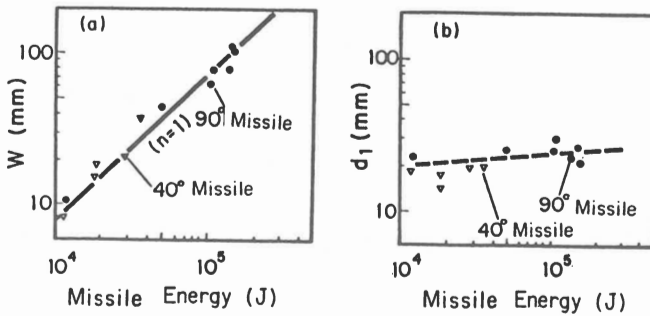Fig. 9   Static compression test method
by a conical indenter.

Fig.10   Maximum residual deflection in target, W, subjected to
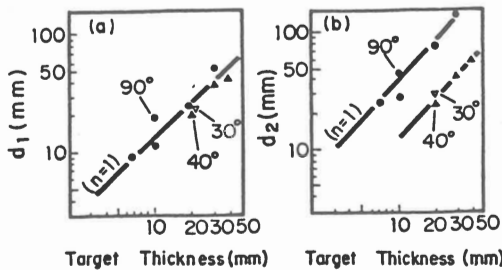conical missile impact, and flat shape diameter, d_1.

Fig.11   Diameters d_1 and d_2 dependence on target
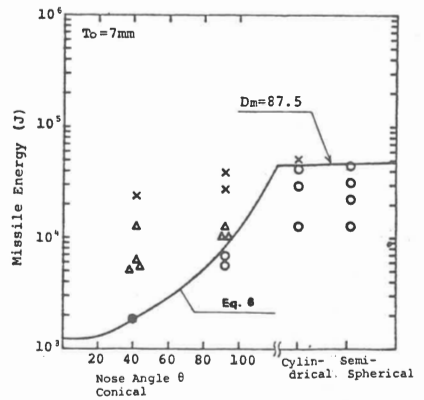thickness T and conical nose angle θ.

Fig.12   Comparison between Eq. (6)
and test results for a 7 mm
thick target plate.